

THE 2018-2019 NEWDIGATE, SURREY, UK EARTHQUAKE SEQUENCE: INDUCED BY NEARBY OILFIELD DEVELOPMENT/PRODUCTION, OR NOT?

Stephen HICKS¹, James VERDON², Brian BAPTIE³, Richard LUCKETT³, Zoe MILDON⁴, THOMAS GERONON⁵

Abstract: *In the UK, induced and triggered earthquakes by hydrocarbon extraction has is an important issue. Starting in April 2018, a sequence of small earthquakes (max. $M_L = 3.0$) occurred in Surrey, close to Gatwick Airport. These events occurred at shallow depth (<3 km) and within 8 km and 3 km of oilfield production and development wells, respectively. As a result, this sequence attracted attention from the public and media, making it important to characterise this sequence in detail. In July, the British Geological Survey installed five seismic stations to better constrain the earthquake characteristics. We performed a template-matching technique to detect ~100 earthquakes in the sequence (min. $M_L = -1.4$), with a mean depth of 2.5 km - below the oil formation targets. Using 2-D seismic profiles, we have identified the causative fault with a normal sense of offset within sedimentary rocks at the base of the Weald Basin. We computed a moment tensor which shows a right-lateral faulting mechanism, consistent with the regional state of the stress. We also computed stress drops and inter-event static stress changes to help discriminate between natural and induced causes. Although there is a curious temporal correlation with extraction and injection at the nearby production well, there is no plausible mechanism for fluid to have migrated across several fault blocks within a short time period. We interpret that the Newdigate earthquakes were not induced. This sequence emphasises the need to further monitor and understand baseline seismicity at shallow depths close to hydrocarbon operations.*

Introduction

Seismicity induced and triggered by industrial activities has recently become a topic of great scientific and public interest around the world (e.g. Ellsworth 2013). Seismic events that occur close to industrial facilities often alarm local communities, yet attributing the cause of an earthquake to a human activity and discriminating between anthropogenic and natural seismicity is not a trivial task (Grigoli et al. 2017). Most research surrounding induced seismicity, particularly wastewater injection, has focussed on stressing faults in the crystalline basement; however, the response of shallow sedimentary rocks to even small changes in induced fluid pressure is poorly understood. Recently, Goebel and Brodsky (2018) showed that as well as earthquake triggering in the basement, injecting fluid into sedimentary units may trigger larger earthquakes occurring at greater distances from the injection site because of poro-elastic effects. Overall, the mechanisms of very shallow earthquakes are not well studied. Conversely, anomalous seismic swarms occurring at shallow depth have been shown to be caused by natural processes (e.g. Bent et al. 2017). Even natural earthquakes occurring close to industrial sites raise strong public concern and can cause financial loss to hydrocarbon operating companies, as shown by the 2015 M_w 6.1 Emilia, Italy earthquake (Dahm et al. 2015; Grigoli et al. 2017). Criteria to discriminate induced versus natural seismicity includes answering qualitative questions (e.g. Davis & Frohlich 1993), and more quantitative analyses such as numerical modelling and statistical tests (Grigoli et al. 2017).

One such example is a sequence of small earthquakes that began in April 2018 close to the village of Newdigate in Surrey, UK (Figure 1). To date, the British Geological Survey (BGS) had detected approximately 30 earthquakes with magnitudes ranging from M_L 3.1 down to M_L -0.2. Nearby residents felt many of the earthquakes in the area, which has a relatively high population, with nearby large settlements including Crawley, Dorking, and Gatwick Airport. From the largest

¹ Imperial College London, London, UK, s.hicks@imperial.ac.uk

² University of Bristol, Bristol, UK

³ British Geological Survey, Edinburgh, UK

⁴ University of Plymouth, Plymouth, UK

⁵ University of Southampton, Southampton, UK

event of the sequence, (M_L 3.1), many people living nearby described a level of shaking corresponding to a maximum intensity of 5 (Strong shaking) on the European Macroseismic Scale (Grünthal 1998). The sequence attracted much public interest for several reasons. First, the area of south-eastern and southern England has historically had a low rate of seismicity (Musson & Sargeant 2007) with very few cases of similar earthquake swarms in the past (Figure 1)). Second, oilfield development and production activities at the active fields of Brockham and Horse Hill lie within 10 km distance of the earthquake sequence (Figure 2). Third, whilst regulators have currently not permitted any licenses in Surrey for hydraulic fracturing, if industrial activities had induced the earthquakes, many events will have had magnitudes well above the UK's current regulatory "red" level for hydraulic fracturing. However, the nearest permanent station of the BGS seismic network lies on the southern coast of England, over 50 km away (Figure 1). This network sparsity made it difficult to determine accurate hypocentres for the earthquakes, particularly depth and faulting mechanism, which can help to discriminate between natural and induced causes (e.g. Frohlich *et al.* 2016). Operational BGS locations for these earthquakes showed a shallow depth (initially fixed to 5.0 km), supported by macroseismic observations, raising suspicions over possible induced causes.

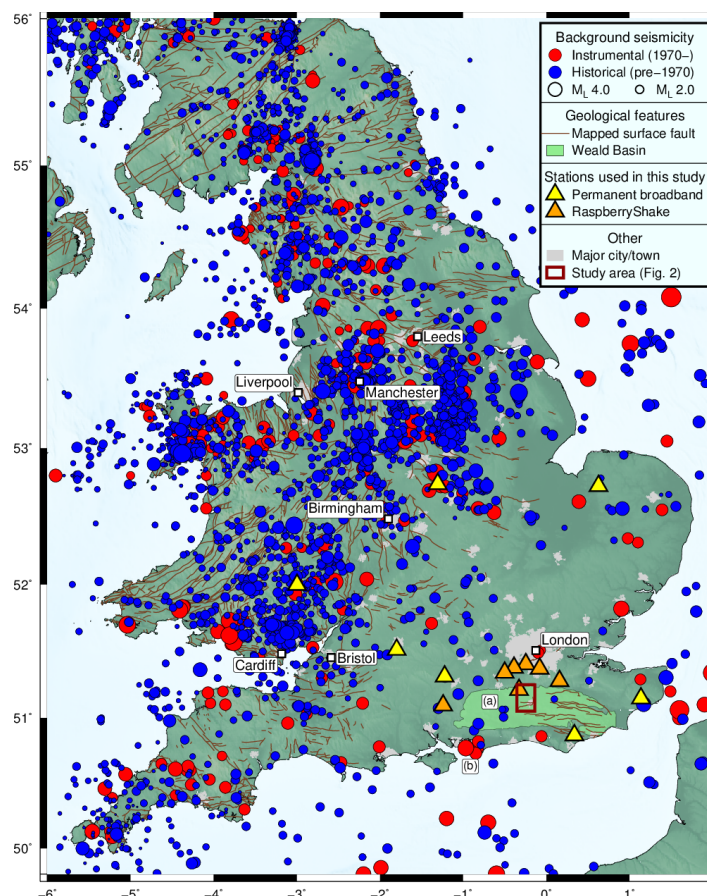


Figure 1: Regional context showing the study area (brown rectangle), together with instrumental and historical seismicity context of England and Wales from the BGS catalogue. Regional seismic stations used in this study are shown. Mapped surface fault traces come from BGS. Labels a) and b) refer to the 2005 Billingshurst and 1811-1834 Chichester sequence, respectively, which are discussed in the text.

Seismic data and event detection / relocation

Following the first nine events of the swarm, the BGS, together with the University of Southampton, installed a network of five temporary stations in the area (Figure 2) comprising Guralp 3ESPC 30 s – 50 Hz seismometers. We installed the first two of these stations (GB.HORS and GB.RUSH) on 12/07/18 and the final three stations (GB.GATW, GB.STAN, GB.BRD) over the period 31/07/18 - 02/08/18. We re-picked P- and S-wave arrival times from all events in the BGS catalogue, classifying the error on each pick because of arrival time uncertainty from 0 to 4

(where 0 shows the smallest error of ~ 0.1 s and 4 is the largest error of > 1.5 s). We performed iterative picking and initial relocation of events using the SDX software package.

We need a robust velocity model for well-constrained earthquake locations, and to make sure no systematic errors bias the hypocentral locations. A 1-D seismic velocity model should represent the average structure along each seismic ray-path, especially close to the source. We based our initial 1-D velocity model on constraints from the BGS's "General UK" operational model and the CRUST1.0 model (Laske *et al.* 2013) for south-east England. We then improved this using sonic logs from the Brockham (UKOGL 2019) and Horse Hill wells (UKOG, personal communication). We tried different layer thicknesses and seismic velocity perturbations in terms of the stability of event locations, spatial clustering of events, and the average residual between observed and theoretical seismic wave arrival times. We also experimented with including a depth-varying S-wave velocity model based on Poisson's ratio constraints at the nearby Balcombe Well (UKOG, personal communication). Overall, we found that a depth-varying shear-wave velocity resulted in higher arrival time residuals, so we used a constant v_p/v_s ratio of 1.73, as per the BGS operational model, which is consistent with Wadati plot analysis.

To relocate the earthquakes, we used NonLinLoc (Lomax *et al.* 2009), which offers a better constraint on location uncertainties compared with traditional single-event location codes. The equal differential time likelihood function implemented by NonLinLoc is very robust in the presence of outliers. It makes the automatic identification of false picks easier, discarding or down-weighting these during calculations if enough phases are present. The posterior probability density function (PDF) as computed by NonLinLoc offers a complete probabilistic solution to the earthquake location problem, independent of initial starting locations, and including information on uncertainty and resolution.

To detect any further events not in the BGS catalogue, we used two approaches. (1) we used the Lassie software, which is a stack- and-delay-based coherence detector to find and locate events using continuous data from the temporary seismic network. Coherency is mapped using smooth characteristic function calculated from normalised waveform envelopes. From events in this catalogue, we then (2) ran a cross-correlation template-matching algorithm on local stations. For this, we used 0.8 s-long template waveforms incorporating P- and S-waves from the events in the catalogue. We used the EQcorrscan package (Chamberlain *et al.* 2018) to scan for similar detections on continuous data filtered at 5-15 Hz. Events are then detected when the network-stacked cross-correlation sum exceeds a threshold of 9 times the Median Absolute Deviation (MAD). We then manually assessed automatic detections, and re-picked and located, where necessary.

Results

In addition to the events recorded in the BGS catalogue, our template matching approach carried out on data from local stations resulted in the detection of a further ~ 70 micro-earthquakes from 2018-07-12 onwards, with magnitudes as low as ML -1.4., forming an overall catalogue of 102 events. We found that even with an appropriate velocity model, local RaspberryShake stations, and our relocation strategy, events that occurred before the installation of the dedicated local network had poorly constrained hypocentre parameters, with depths ranging from 0 km to 2.4 km and mean depth uncertainties of ± 1.5 km. Because of this inherent uncertainty for the earlier events in the sequence, we first focussed on the 17 events that all five local temporary stations had recorded. Our hypocentre solutions for these well-constrained events had a mean depth of 2.3 km below sea level, with most having formal epicentral and depth uncertainties of ~ 500 m and < 800 m, respectively. We found that these solutions were robust as they varied little when we tested different velocity models and had low RMS arrival time residuals (< 60 ms). Overall, these best constrained events indicated a source area ~ 1.6 km long and 1.0 km in depth. For the events recorded by only two temporary stations, we found that inclusion of stations at longer epicentral distances (> 25 km) resulted in poorly constrained depths, even though we applied a distance weighting to observations in the relocation strategy (e.g. Theunissen *et al.* 2018).

The temporary stations captured five of the larger events of the sequence in July 2018 and February 2019, providing a unique opportunity to probe rupture mechanisms, and to independently constraint on source depth using waveform inversion. Figure 4 shows the results of the moment tensor inversion. All five events have a best centroid depth of 2.0 ± 0.2 km and show a similar strike-slip faulting mechanism, comprising either right-lateral faulting along a west-east striking fault plane dipping steeply to the north or left-lateral faulting along a north-south

striking fault plane. The retrieved double-couple percentage is high for all events (>90%), regardless of the limited station coverage for the July events, which may artificially reduce double-couple components (e.g. Sileny 2009).

Our results from hypocentral relocation and moment tensor inversions suggest a consistent depth range of 1.8–2.4 km. Therefore, we fixed the depths of the events that occurred before 2018-08-12 to 2.1 km (Figure 2). The high waveform similarity and cross-correlation values between the largest events in the sequence (waveform cross-correlation >0.80 for a 0.7 window including the P-wave arrival supports this assumption. Overall, most event epicentres from our full catalogue appear to cluster along a roughly linear band, trending approximately east-west (Figure 2).

In Figure 2, we examine whether this cluster of earthquakes correlates with pre-existing faults identified from 2-D seismic profiles. Many of these faults strike east-west and dip towards the south, although we also infer north-dipping and ENE–WSW trending faults. The Newdigate Fault (NGF) is a prominent east-west striking, south-dipping fault structure showing a normal sense of offset, which extends across much of the study area. Most earthquake epicentres lie along the projected surface trace of the NGF, suggesting that the Newdigate sequence occurred along this fault or a related structure. In cross-section, the NGF comprises multiple strands, with the main fault offsetting horizons by ~50 m. We can trace this fault from just below the surface to over 2.5 km depth. Away from the NGF, we also find one or two small events (ML <0.0) with well-constrained locations that correspond to the inferred surface trace of the NE-SW striking Horse Hill Fault (HHF), which dips to the north-west (Figure 2).

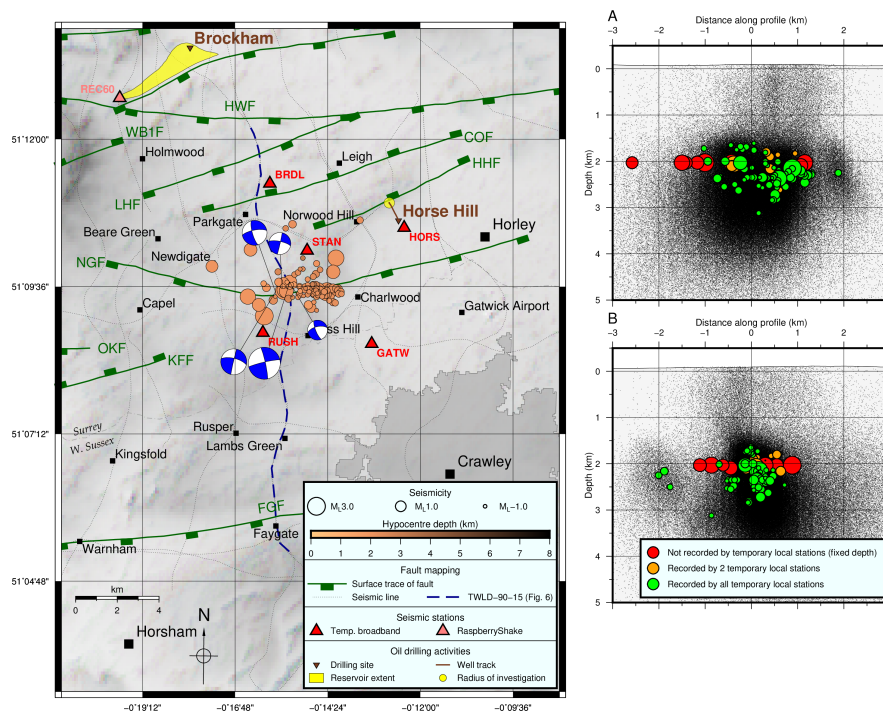


Figure 2: Left: map of the study area showing relocated earthquakes of the 2018-2019 Newdigate sequence, focal mechanisms, mapped faults, local seismic stations, and the locations of oilfield activities. Only high-quality earthquake hypocentres are plotted with a maximum azimuthal gap of 200°. Right: cross-sections of seismicity with event hypocentres and combined scatter density clouds to represent the hypocentre probabilistic density functions. The cross-section locations are labelled on the map. The definition of fault abbreviations are as follows: BHF = Box Hill Fault; BRF = Brockham Fault; BUF = Buckland Fault; COF = Collendean Fault; FGF = Faygate Fault; HWF = Holmwood Fault; HHF = Horse Hill Fault; KFF = Kingsfold Fault; LHF = Leigh Fault; NGF = Newdigate Fault; OKF = Ockley Fault; WCF = Westcott Fault; WB1F = Whiteberry-1 Fault.

Discussion

On the basis of the location of our interpreted subsurface faults and earthquake locations, we identify the Newdigate Fault as the causative structure for most of the earthquakes in the Newdigate sequence. Given this correlation, and the computed moment tensors, it is most likely

that the earthquakes represent right-lateral strike slip faulting along this west-east striking structure. The hypocentre and moment tensor centroid depths support a ~2 km mean focal depth of the earthquakes, showing that the earthquakes likely occurred within the Middle-Lower Jurassic to Upper Triassic sedimentary rocks of the Weald Basin. At these depths, and according to interpreted well logs from Horse Hill and Brockham, the rock types are mainly mudstone-rich, although the conceivably stronger limestone unit of the Penarth Formation at ~2.3 km depth could promote the brittle failure required for seismic slip.

Using the Frohlich *et al.* (2016) criteria, although there is some uncertainty arising from the testing the questions posed, we could classify the Newdigate sequence as either “Possibly Induced” or “Probably Induced”. However, this approach is likely an over-simplification as it does not consider detailed source parameters or knowledge of fluid pressure and/or fluid pathways, and is also representative of the inherent bias in the Frohlich *et al.* (2016) criteria, whereby answering all 5 questions with “not sure” and awarding 0.5 points gives an overall answer of “Probably Induced”.

The faulting mechanisms for the larger events of the Newdigate sequence (Figure 2) are consistent with the overall pattern in the British Isles, in which strike-slip faulting dominates with a similar sense of slip (Baptie 2010). This comparison shows that the Surrey earthquakes are consistent with the regional stress field of northwest-southeast compression. These pre-existing east-west trending faults have an optimal orientation for reactivation in the UK’s NW-SE regional stress field. None of our moment tensor solutions show a large non-double-couple component, which other studies have associated to induced earthquakes (Wang *et al.* 2018; Šílený *et al.* 2009). The lack of a strong extensional component to the computed focal mechanisms shows that a compaction/subsidence mechanism did not cause the Newdigate earthquakes; such mechanisms can occur in the overburden above depleted hydrocarbon reservoirs (Van Wees *et al.* 2014; Ottemöller *et al.* 2005; Dahm *et al.* 2015).

Conclusions

Based on the available evidence and consideration of possible triggering mechanisms, we conclude that it is very unlikely that anthropogenic activities induced the 2018-2019 Newdigate seismic sequence. The main line of evidence that could point to the start of this earthquake sequence being induced is the temporal correlation with a restart of production and injection activities at Brockham following a two-year pause. However, we find that the low net extraction in the Brockham reservoir is very unlikely to have caused substantial stress variations over ~8 km distance, and the numerous east-west trending faults in the region act as a fluid permeability barrier. Development work at the nearby Horse Hill well involved very small levels of extraction and injection over a short period in 2016, well before the first earthquake. Further production at Horse Hill from July 2018 onwards occurred while the earthquake sequence was already underway. Similarly, with the seismicity lying ~3 km away without an obvious structural connection, and the relatively small volumes involved, we find it is unlikely for the Horse Hill development operations to have triggered a further uptick in seismicity in 2019. If such a triggering mechanism exists, it is likely to be very subtle and may not be discernible from the available data. Recent work (e.g. Goebel and Brodsky (2018) show that fluid injection into sedimentary sequences can trigger larger earthquakes over greater distances compared to basement injection. However, based on the case studies in that paper in which magnitude 2-3 earthquakes were triggered, the net volume of fluid injected at Brockham and Horse Hill remains virtually negligible below these past cases of high volume and high rate injection.

Our study has shown that natural seismic activity can occur at shallow depths in UK sedimentary basins, especially where pre-existing faults exist that have an optimal orientation for reactivation in the regional stress field. This result has implications for understanding the background rate of seismicity close to hydrocarbon exploration targets. Such shallow seismicity could pose a moderate seismic hazard to areas of high population density. In agreement with Anthony *et al.* (2018), we conclude that citizen seismology networks are suitable for densifying and complementing existing backbone networks for the study of shallow local earthquakes.

References

- Anthony, R.E. *et al.*, 2018. Do Low-Cost Seismographs Perform Well Enough for Your Network? An Overview of Laboratory Tests and Field Observations of the OSOP Raspberry Shake 4D. *Seismological Research Letters*, 90(1), pp.219–228.

- Baptie, B., 2010. Seismogenesis and state of stress in the UK. *Tectonophysics*, 482(1-4), pp.150–159.
- Bent, A.L. et al., 2017. The McAdam, New Brunswick, Earthquake Swarms of 2012 and 2015–2016: Extremely Shallow, Natural Events. *Seismological Research Letters*, 88(6), pp.1586–1600.
- Chamberlain, C.J. et al., 2018. EQcorrscan: Repeating and Near-Repeating Earthquake Detection and Analysis in Python. *Seismological Research Letters*, 89(1), pp.173–181.
- Dahm, T. et al., 2015. Discrimination between induced, triggered, and natural earthquakes close to hydrocarbon reservoirs: A probabilistic approach based on the modeling of depletion-induced stress changes and seismological source parameters. *Journal of Geophysical Research: Solid Earth*, 120(4), pp.2491–2509.
- Davis, S.D. & Frohlich, C., 1993. Did (Or Will) Fluid Injection Cause Earthquakes? - Criteria for a Rational Assessment. *Seismological Research Letters*, 64(3-4), pp.207–224.
- Ellsworth, W.L., 2013. Injection-Induced Earthquakes. *Science*, 341(6142), pp.1225942–1225942.
- Frohlich, C. et al., 2016. A Historical Review of Induced Earthquakes in Texas. *Seismological Research Letters*, 87(4), pp.1022–1038.
- Goebel, T.H.W. & Brodsky, E.E., 2018. The spatial footprint of injection wells in a global compilation of induced earthquake sequences. *Science*, 361(6405), pp.899–904.
- Grigoli, F. et al., 2017. Current challenges in monitoring, discrimination, and management of induced seismicity related to underground industrial activities: A European perspective. *Reviews of Geophysics*, 55(2), pp.310–340.
- Grünthal, G., 1998. *European macroseismic scale 1998*, European Seismological Commission (ESC).
- Laske, G. et al., 2013. Update on CRUST1. 0—A 1-degree global model of Earth's crust. In *Geophys. Res. Abstr. EGU General Assembly Vienna, Austria*, p. 2658.
- Lomax, A., Michelini, A. & Curtis, A., 2009. Earthquake location, Direct, Global-search Methods. In R. A. Meyers, ed. *Encyclopedia of complexity and systems science*. Encyclopedia of Complexity and Systems Science. New York, NY: Springer New York, pp. 2449–2473.
- Musson, R. & Sargeant, S.L., 2007. Eurocode 8 seismic hazard zoning maps for the UK.
- Ottmøller, L. et al., 2005. The 7 May 2001 induced seismic event in the Ekofisk oil field, North Sea. *Journal of Geophysical Research: Solid Earth (1978–2012)*, 110(B10), p.379.
- Sileny, J., 2009. Resolution of Non-Double-Couple Mechanisms: Simulation of Hypocenter Mislocation and Velocity Structure Mismodeling. *Bulletin of the Seismological Society of America*, 99(4), pp.2265–2272.
- Šílený, J. et al., 2009. Non-double-couple mechanisms of microearthquakes induced by hydraulic fracturing. *Journal of Geophysical Research: Solid Earth (1978–2012)*, 114(B8), p.677.
- Theunissen, T. et al., 2018. Absolute earthquake locations using 3-D versus 1-D velocity models below a local seismic network: example from the Pyrenees. *Geophysical Journal International*, 212(3), pp.1806–1828.
- UKOGL, 2019. UK Onshore Geophysical Library. Available at: <https://ukogl.org.uk> [Accessed January 1, 2019].
- Van Wees, J.D. et al., 2014. Geomechanics response and induced seismicity during gas field depletion in the Netherlands. *Geothermics*, 52, pp.206–219.
- Wang, R. et al., 2018. Faults and Non-Double-Couple Components for Induced Earthquakes. *Geophysical Research Letters*, 45(17), pp.8966–8975.